Desalination and Water Treatment
www.deswater.com

doi: 10.5004/dwt.2017.21399

90 (2017) 311–319
September

Examination of the adsorption for methylene blue using different adsorbents

Çiğdem Sarıcı-Özdemir

Department of Chemical Engineering, Faculty of Engineering, Inonu University, 44280 Malatya, Turkey, Tel. +90 422 3774757; Fax: +90 422 3410046; email: cigdem.ozdemir@inonu.edu.tr

Received 25 January 2017; Accepted 29 August 2017

ABSTRACT

This study was conducted on methylene blue adsorption using adsorbents obtained in different ways. These adsorbents were divided into four groups among its members. Activated carbon obtained after chemical activation, clay, industrial waste and agricultural waste constitutes this group. Adsorbents were characterized by X-ray diffractometer, scanning electron microscopy and Fourier-transform infrared spectroscopy. The adsorption of methylene blue onto adsorbents was investigated by calculating the parameters of contact time, the concentration of methylene blue and adsorbent dosage. Experimental data obtained from dye adsorption were studied by five two-parameter (Langmuir, Freundlich, Dubinin–Radushkevich, Temkin and Frumkin), five three-parameter (Redlich–Peterson, Sips, Toth, Radke–Prausnitz, Koble–Corrigan) isotherm models. The Langmuir and Freundlich model denotes a better value of correlation coefficient than other models. The amount of methylene blue adsorption at equilibrium by the adsorbents showed the following order; clay > activated carbon > fly ash > pine cone. Maximum adsorption capacity for methylene blue was calculated 250 mg g^{-1} at clay.

Keywords: Activated carbon; Adsorption; Wastes; Methylene blue

1. Introduction

The technology is changing quickly and evolving depending on the growing needs of mankind. This development brings problems such as environmental pollution. A few hundred pollutants were found to contaminate water resources. These pollutants have a high toxicological effect. Various treatment technologies including flocculation, coagulation, biological oxidation, sedimentation, adsorption and combined methods are applied to collect pollutants from wastewater [1]. Research on the treatment of wastewater containing dyes revealed that adsorption was a highly effective technique for removing wastewater from dyes [2]. Adsorption is generally considered to be an effective and economical method. A selective feature is the main advantage of removing hazardous substances due to functional groups on the surface of the adsorbent [3]. The adsorbent used in adsorption has an important effect. Low cost, easy to find efficiency, pore structure and many other properties are important for the use of adsorbent. Mittal et al. [4] a new adsorbent, PMMA-gft-Alg/Fe_3O_4, was synthesized by an oxidative-free radical graft copolymerization reaction and was evaluated for the removal of Pb(II) and Cu(II) from aqueous solutions.

The high surface area of active carbon, microporous character and surface chemical structure make it highly efficient as a potential adsorbent. Fly ash (FA) is a by-product of coal combustion occurring in various industrial processes. The fact that coal is used as a fuel in most industries causes FA to be produced in higher amounts, and this, in turn, causes many problems. The abovementioned factors restrict the usage of FA in industries [5]. Clay minerals, especially the smectite family, have received considerable attention owing to their physicochemical properties and high capacity to retain organic compounds [6]. Pine is a suitable tree for decorative planting in nature. Thus, ground pinecone may be abundantly available. It would be worthwhile to develop a low-cost adsorbent from this waste material which may also be regarded as a sustainable resource, since the trees themselves do not have to be harvested [7].

The objective of this research is to investigate the capability of activated carbon (AC), clay, FA and pine cone (PC) for adsorption of methylene blue (MB) from aqueous solution.

1944-3994/1944-3986 © 2017 Desalination Publications. All rights reserved.

The effect of adsorbents with different surface properties on MB adsorption will be examined. In this study, the AC was prepared by subjecting wastes to a process of chemical activation in the absence of nitrogen (N_2) at 500°C. The clay (CL) was obtained from Malatya region. Hydrothermal power plant waste FA has been used as adsorbent. The campus site was used as a source of PC obtained from agricultural waste containing adsorbent.

2. Experimental

2.1. Adsorbent preparation

Textural waste, provided from GAP A.Ş. in Malatya, Turkey, was used in this study as a source of AC. Poly(ethyleneterephthalate) is to form 90% of the textural waste. The raw materials were subjected to two steps of activation as follows:

- The raw material was mixed with K_2CO_3 the ratio of 1:1 (w/w, K_2CO_3/starting material), and the mixture was kneaded by adding distilled water. The mixture was then dried at 110°C to prepare the impregnated sample.
- The impregnated sample was placed on a quartz dish, which was then inserted within a quartz tube (internal diameter = 60 mm). The impregnated sample was heated at the rate of 10°C min^{-1} up to the activation temperature (500°C) under N_2 flow (100 mL min^{-1}) and held at the activation temperature for 1 h. After activation, the sample was cooled under N_2 flow. The sample was washed sequentially several times with hot distilled water to remove any residual chemical and until a pH of 7 was reached. The washed sample was dried at 110°C to prepare AC.

FA, provided by Afsin-Elbistan Thermal Reactor in Kahramanmaraş, Turkey. The sample (30 g) was mixed with 0.5 M $ZnCl_2$ (50 mL) at room temperature for 24 h. The sample was washed several times with hot distilled water to remove any residual chemicals and reached a pH of 7. The washed sample was dried at 110°C to prepare adsorbent. The clay was provided in Malatya, Turkey. The clay and PC were milled and sieved under 200 mesh. FA, CL and PC were dried at 110°C to prepare adsorbent.

2.2. Materials

MB was used as adsorbate in this work. MB is a cationic dye. MB has the molecular formula $C_{16}H_{18}N_3SCl$ and the molecular weight of 319.85 g mol^{-1}. MB was supplied by Merck. The spectrophotometric determination of MB was carried out using a Shimadzu UV/Vis spectrophotometer in 662 nm. Measurement in 5 mL of cuvettes was used.

2.3. Adsorption experiments

The MB solution was prepared in distilled water at the desired concentrations. Adsorption experiments were carried out by agitating 0.1 g of adsorbent with 50 mL solutions of the desired concentration (25–125 mg L^{-1}) at 25°C and a thermostatic bath operating at 400 rpm. The amount of dry adsorbed onto adsorbent, q_t(mg g^{-1}) was calculated by the mass balance relationship, as shown in Eq. (1):

$$q_t = (C_0 - C_t)\frac{V}{W} \tag{1}$$

where C_0 and C_t are the initial and time 't' liquid-phase concentrations of the dry material (mg L^{-1}), respectively. V is the volume of the solution (L), and W is the weight of the dry adsorbent used (g).

In order to quantitatively compare the applicability of isotherm equations in fitting to data, non-linear correlation coefficient and relative error, Δq, were calculated.

$$\Delta q = \sqrt{\frac{\sum\left[(q_{t(\exp)} - q_{t(\mathrm{cal})}) / q_{t(\exp)}\right]^2}{n-1}} \times 100 \tag{2}$$

where n is the number of data points; $q_{t(\exp)}$ is the experimental values; and $q_{t(\mathrm{cal})}$ is the calculated values by the isotherm.

3. Results and discussion

3.1. Adsorbent characterization

Scanning electron micrographs are important in the characterization of adsorbent. Here the porosity and secondary structures are determined. Scanning electron microscopy (SEM) graphs of the adsorbent are shown in Fig. 1. Micrographs also show the heterogeneity of the surface of the produced AC (Fig. 1(a)) and the irregular distribution of pores. The polymer shape used in the production of the AC fiber structure is observed. Under microscopic examination, FA (Fig. 1(b)) blend shows a rough non-uniform surface with highly shrunken pores. In addition, the image clearly proves that FA and $ZnCl_2$ have a perfect blend without forming any coagulates. The clay minerals can crystallize in a more stable structure since big-size pores favor the growth of clay minerals. The morphology of illite in sandstones presents fiber-like (fibrous) and hair filament aspects under the SEM. Illite–montmorillonite shows aggregates of flakes, short filaments, honeycomb-like and palmate. Kaolinite presents a book-like structure and exhibits a hexagonal tabular form. CL showed that the illite and chlorite pores are similar, and essentially meso–macro pores in Fig. 1(c) [8]. PC has got micropore from Fig. 1(d).

The studied samples were characterized by XRD (Rigaku Geigerflex D/MaxB) (Fig. 2). AC has amorphous structure between 2θ = 20 and 30 ranges. The XRD pattern of clay (Fig. 2) shows prominent peaks assigned to kaolinite, quartz. The rays of many minor minerals (anatase, rutile, goethite, maghemite and pyrite) overlap with those of major minerals such as kaolinite, quartz and montmorillonite [9]. The XRD pattern of FA is presented in Fig. 2. The major mineral compositions of FA are lime (f-CaO), calcite ($CaCO_3$), calcium hydroxide ($Ca(OH)_2$) and anhydrite ($CaSO_4$) [10]. The results in Fig. 2 show the XRD pattern of PC. The characteristic main peaks of cellulose at the 2θ of 19.8° and 34° can be observed. These peaks are indicative of highly organized crystalline cellulose.

The FTIR (Mattson 1000) spectrum of adsorbents is presented in Fig. 3. FTIR spectrum of AC shows many peaks belonging to different functional groups. The peak at 3,000 cm^{-1} belongs to aliphatic C–H bonds. The peak that appears at 3,625 cm^{-1} indicates free –OH structure. In the case of clay with an aliphatic structure, this is seen at a peak at

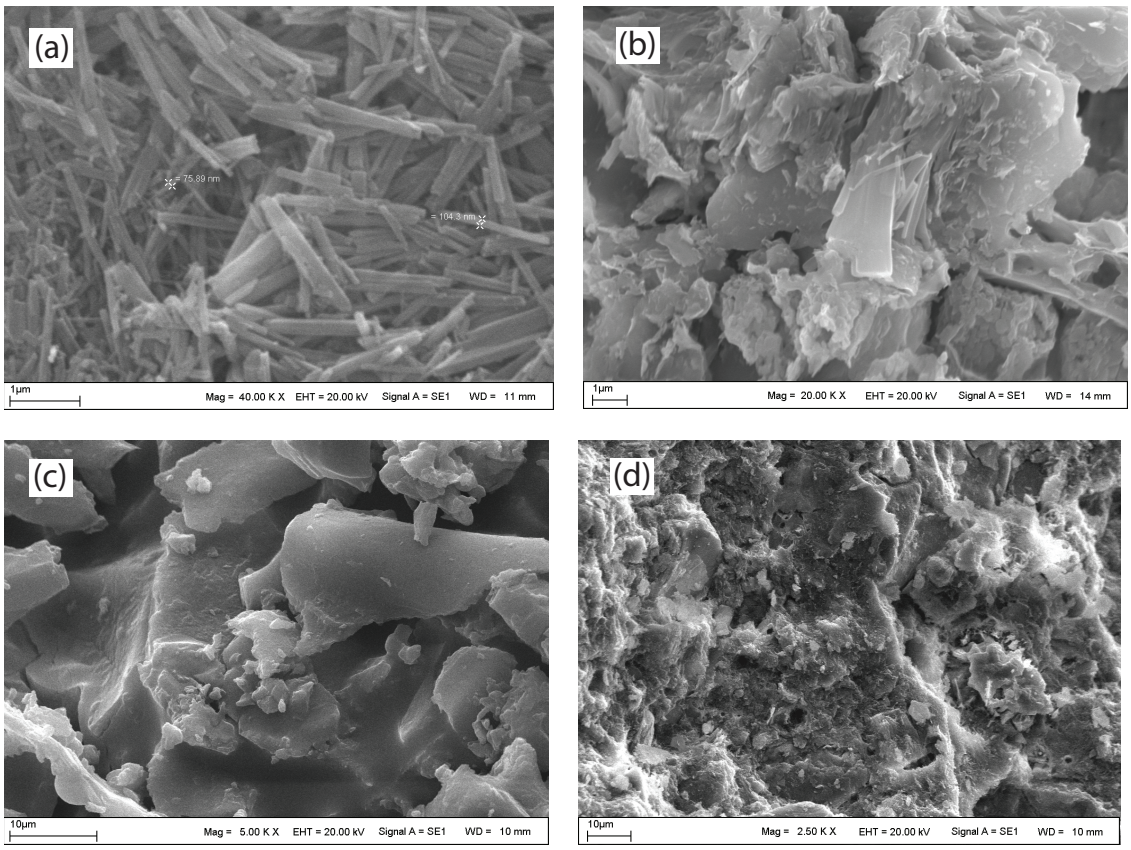

Fig. 1. Scanning electron micrographs of adsorbents (a) AC, (b) FA (c) CL (d) PC.

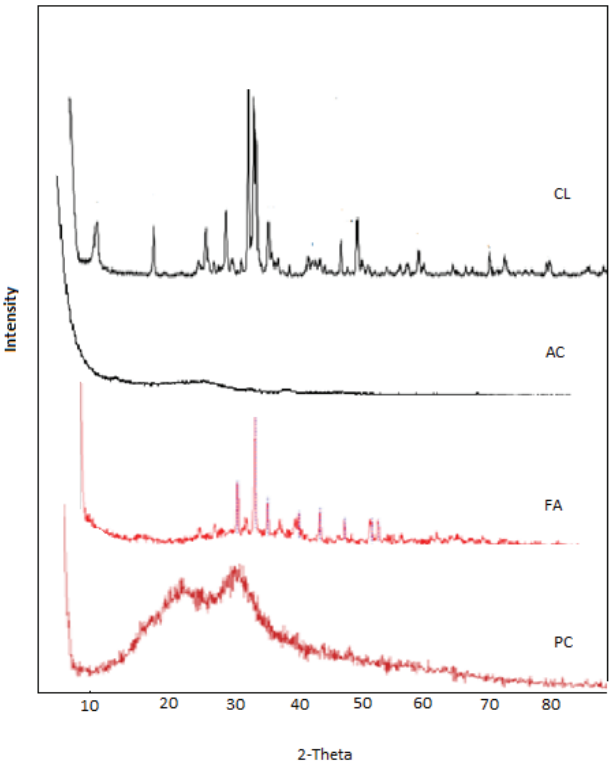

Fig. 2. X-ray diffractograms of adsorbents.

3,200 cm^{-1}. Within the structure, the peak belonging to the carbonate group is around 1,400 cm^{-1} and the peak belonging to the lactones is around 1,800 cm^{-1}. Asymmetric Si–O peak is observed at 800 cm^{-1}. FTIR spectrum of PC shows strong aliphatic structure at 3,000 cm^{-1}. The Si–O–Si structure at 1,000 cm^{-1}, with fewer functional groups for FA.

3.2. Investigation of adsorption parameters

3.2.1. Effect of initial concentration of MB

The effect of initial concentration of MB on its removal from the aqueous solutions by AC, CL, FA and PC was studied as shown in Fig. 4. It has been found that the percentage of dye cleaning decreases with increasing initial dye concentration for all adsorbents. This shows that increasing initial dye concentrations reduce the adsorption to the adsorbents due to the absence of active areas present on the surface of the adsorbents. The effect of initial MB concentration on adsorption has been determined at concentrations ranging from 25 to 125 mg L^{-1} at 25°C. Fig. 3 shows the maximum adsorption that almost 95%, 89%, 95%, 99% of adsorbed dye at 25 mg L^{-1} for AC, CL, FA and PC, respectively. These different percentages of adsorption are due to the difference in the surface properties of the adsorbents. Depending on the superficial pore structure, this reduction was faster in the clay and PC. Maximum adsorption that almost 82%, 86.5%, 71%, 72% of MB are adsorbed at 125 mg L^{-1} for AC, CL, FA and PC, respectively.

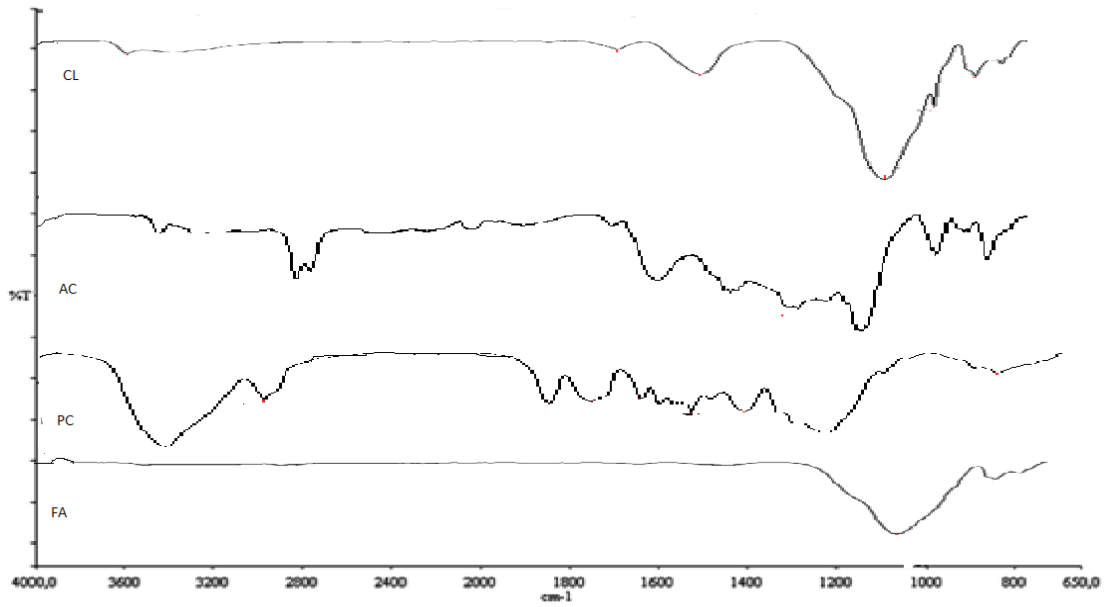

Fig. 3. FTIR diffractograms of adsorbents.

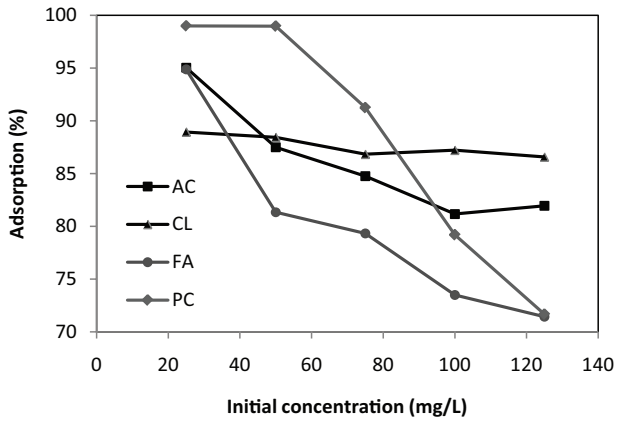

Fig. 4. Effect of initial concentration of dye.

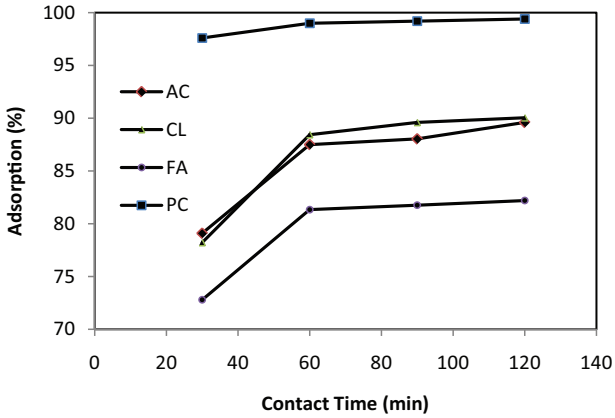

Fig. 5. Effect of contact time.

3.2.2. *Effect of contact time*

The effect of contact time for removing MB from aqueous solutions with AC, CL, FA and PC was studied as shown in Fig. 5. The percentage removal of dye is found to increase with increase in contact time for all adsorbents. However, the fastest growth was seen crossing from 30 to 60 min. After 60 min, there will not be much change. Therefore, adsorption equilibrium studies were performed for 60 min. The removal of MB is rapid in the initial stages of contact time and gradually decreases with lapse of time until saturation. The removal curves are single, smooth and continuous, indicating monolayer coverage of dye on the outer interface of the adsorbent initially.

3.2.3. *Effect of adsorbent dosage*

The effect of adsorbent dosage for MB adsorption from the aqueous solutions by AC, CL, FA and PC has been studied as shown in Fig. 6. The biggest increase is from 0.05 to 0.1 g (Fig. 6). No significant increase in the dosage of the next adsorbent was observed. This is seen in four different adsorbents we use. The pores in the surface of the adsorbent are filled with saturation for this concentration range.

3.3. *Adsorption isotherms*

In order to determine the mechanism of MB adsorption onto AC, CL, FA and PC, the experimental data were applied to the isotherm of two parameters Langmuir [11], Freundlich [12], Dubinin–Radushkevich [13], Temkin [14], and Frumkin [15] and three parameters Redlich–Peterson [16], Sips [17], Toth [18], Radke–Prausnitz [19], Koble–Corrigan [20] were studied. Table 1 shows the equations and constants of such isotherms.

The constant parameters of the isotherm equations for this adsorption process were calculated by regression using

the linear form of the isotherm equations. The constant parameters and correlation coefficients (R^2) are listed in Table 2. Figs. 7–10 show the experimental equilibrium data as well as the fit to the different isotherm models using the error criterion for MB at AC, CL, FA and PC, respectively.

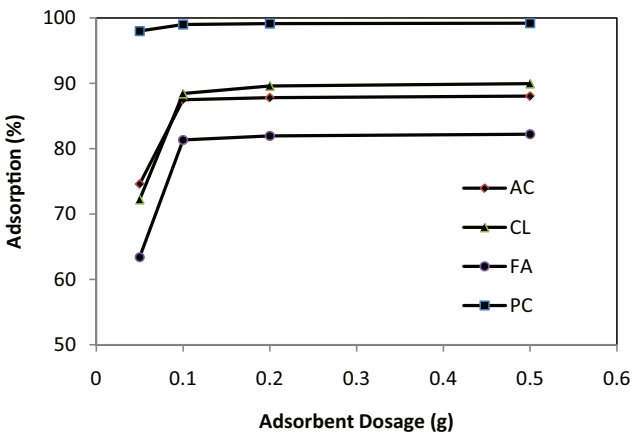

Fig. 6. Effect of adsorbent dosage.

The Langmuir isotherm data are presented in Table 2 for different adsorbent. The adsorption capacities order have been determined for dye as 66.67, 250, 55.56 and 45.46 mg g^{-1} for AC, CL, FA, and PC, respectively. The surface properties of the adsorbents are different. Because of this difference, the adsorption capacities also change. The adsorbent pore size and the molecular size compatibility of the dye were best observed in the CL. Therefore, the adsorption capacity of the clay is the highest. The values of the correlation coefficients for Langmuir isotherm are the highest values when compared with the values obtained for other isotherms for PC. Therefore, Langmuir isotherm is considered as the best-fit isotherm equation for PC (Fig. 10).

Table 2 shows Freundlich adsorption isotherm constants, correlation coefficient and relative error for AC, CL, FA and PC, respectively. The value of n for the Freundlich isotherm was found to be greater than 1; hence, MB was favorably adsorbed by AC, CL, FA and PC. Freundlich isotherm is considered as the best-fit isotherm equation for CL (Fig. 8) [21].

Table 1
List of isotherm equilibrium

Isotherm	Non-linear form	Linear form	Plot
Two parameters			
Langmuir	$q_e = \frac{Q_o b C_e}{1 + bC_o}$	$\frac{C_e}{q_e} = \frac{1}{bQ_o} + \frac{C_e}{Q_o}$	$\frac{C_e}{q_e}$ vs. C_e
Freundlich	$q_e = K_F C_e^{1/n}$	$\ln q_e = \ln K_f + \frac{1}{n}\ln C_e$	$\ln C_e$ vs. $\ln q_e$
Dubinin–Radushkevich	$q_e = (q_m)\exp(-k_{ad}\varepsilon^2)$	$\ln q_e = \ln q_m - k_{ad}\varepsilon^2$	$\ln q_e$ vs. ε^2
Temkin	$q_e = \frac{RT}{b_T}\ln A_T C_e$	$q_e = \frac{RT}{b_T}\ln A_T + \left(\frac{RT}{b_T}\right)\ln C_e$	Q_e vs. $\ln C_e$
Frumkin	$\frac{\theta}{(1-\theta)}e^{-2a\theta} = k.C_e$	$\ln\left[\left(\frac{\theta}{1-\theta}\right).\frac{1}{C_e}\right] = \ln k + 2a\theta$	$\ln\left[\left(\frac{\theta}{1-\theta}\right).\frac{1}{C_e}\right]$ vs. θ
Three parameters			
Redlich–Peterson	$q_e = \frac{K_R C_e}{1 + a_R C_e^{\beta}}$	$\ln\left(K_R\frac{C_e}{q_e} - 1\right) = \beta\ln(C_e) + \ln(a_R)$	$\ln\left(K_R\frac{C_e}{q_e} - 1\right)$ vs. $\ln C_e$
Sips	$q_e = \frac{K_s a_s C_e^s}{1 + a_s C_e^s}$	$s\ln(C_e) = -\ln\left(\frac{K_s}{q_e}\right) + \ln a_s$	$\ln\left(\frac{K_s}{q_e}\right)$ vs. $\ln C_e$
Toth	$q_e = \frac{K_T C_e}{\left(a_T + C_e^t\right)^{1/t}}$	$\ln\left(\frac{q_e}{K_T}\right) = \ln(C_e) - \frac{1}{t}\ln\left(a_T + C_e\right)$	$\ln\left(\frac{q_e}{K_T}\right)$ vs. $\ln C_e$
Radke–Prausnitz	$q_e = \frac{K_{Rp}.k_{Rp}.C_e}{\left(1 + k_{Rp}.C_e^p\right)}$	$\frac{C_e}{q_e} = \frac{1}{K_{RP}.k_{RP}} + \frac{1}{K_{RP}}C_e^p$	$\frac{C_e}{q_e}$ vs. C_e^p
Koble–Corrigan	$q_e = \frac{A.C_e^n}{1 + BC_e^n}$	$\frac{1}{q_e} = \frac{B}{A} + \frac{1}{A}.\frac{1}{C_e^n}$	$\frac{1}{q_e}$ vs. $\frac{1}{C_e^n}$

Table 2
Isotherm constant

	AC	CL	FA	PC
Langmuir				
Q_o (mg g^{-1})	66.67	250	55.56	45.46
b (L mg^{-1})	2.16×10^{-3}	9.62×10^{-4}	3.38×10^{-3}	5.94×10^{-4}
R^2	0.874	0.849	0.909	0.994
Δq (%)	22.57	4.29	29.33	3.62
Freundlich				
K_f (L g^{-1})	10.08	4.62	10.06	21.54
n	2.06	1.15	2.55	4.65
R^2	0.975	0.997	0.961	0.857
Δq (%)	8.88	3.09	10.83	19.51
D-R				
q_m (mol g^{-1}) × 10^3	1.02	8.48	0.55	0.31
K (mol^2 kJ^{-2})	0.003	0.006	0.003	0.001
E (kJ mol^{-1})	12.91	9.12	12.91	22.36
R^2	0.964	0.997	0.946	0.874
Δq (%)	56.79	57.67	14.07	79.05
Temkin				
B_1 (mg g^{-1})	12.30	23.12	9.21	5.64
b (kJ mol^{-1})	201.43	107.16	269	439.29
K_T (L mg^{-1})	1.57	0.51	2.01	69.11
R^2	0.872	0.96	0.872	0.943
Δq (%)	26.88	4.08	35.02	41.71
Frumkin				
a	−5.09	−6.48	−4.22	−5.63
ln$k$	9.19	6.20	9.91	14.06
$-\Delta G$ (kJ mol^{-1})	22.77	15.37	24.55	34.84
R^2	0.720	0.802	0.728	0.859
Δq (%)	23.03	17.69	22.16	17.71
Red.Peterson				
K_R	333.33	25	90.91	200
a_R	32.1	4.43	8.11	7.58
β	0.52	0.149	0.637	0.848
R^2	0.978	0.988	0.981	0.988
Δq (%)	9.21	3.1	11.68	15.32
Sips				
K_S	300	1000	500	250
a_s	0.0295	0.0045	0.0194	0.0822
s	0.5	0.875	0.41	0.25
R^2	0.975	0.997	0.961	0.857
Δq (%)	12.33	6.57	11.77	20.01
Toth				
K_T	41.26	200	33.33	43.47
a_T	4.28	19.92	3.31	2.015
t	0.98	0.99	0.98	0.99
R^2	0.913	0.762	0.961	0.857
Δq (%)	22.33	75.98	24.76	44.91

(Continued)

Table 2 *(Continued)*

	AC	CL	FA	PC
Radke-Pra.				
K_{RP}	9.53	8.33	10.87	32.25
k_{RP}	13.11	1.212	2.19	2.38
p	0.48	0.2	0.6	0.9
R^2	0.965	0.981	0.975	0.998
Δq (%)	10.69	3.01	16.21	16.65
Koble-Corr.				
A	11.12	4.53	11.11	66.67
B	0.04	0.00045	0.044	1.42
n	0.5	0.9	0.4	0.9
R^2	0.983	0.988	0.967	0.937
Δq (%)	10.42	5.38	12.11	14.32

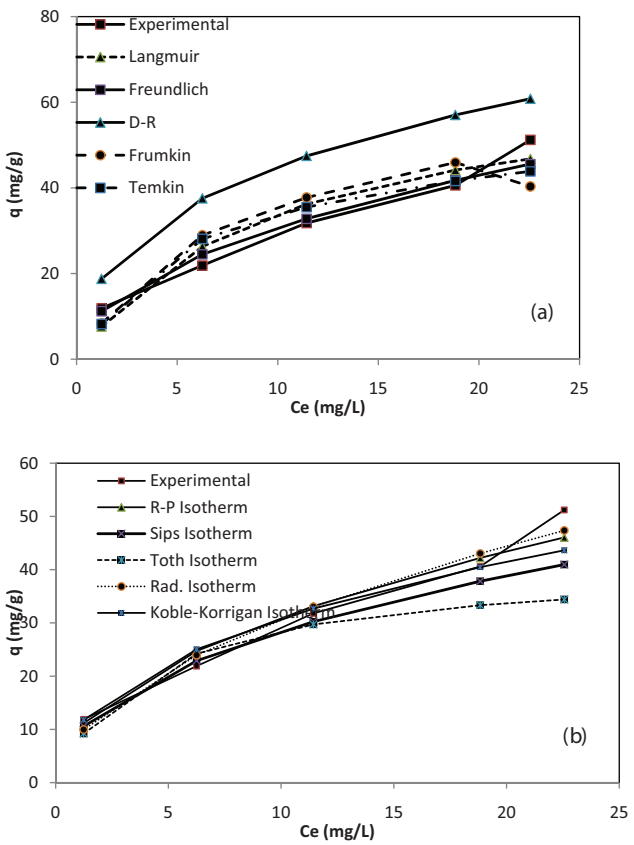

Fig. 7. Adsorption isotherm equations of AC. (a) Two parameters; (b) three parameters.

Dubinin–Radushkevich isotherm is generally applied to express the adsorption mechanism with a Gaussian energy distribution onto heterogeneous surface. The isotherm is usually applied to distinguish the physical and chemical adsorption of ions by the average free energy, which can be calculated by E molecular relationship per adsorbate molecule.

$$E = \left[\frac{1}{\sqrt{2k_{ad}}} \right] \quad (3)$$

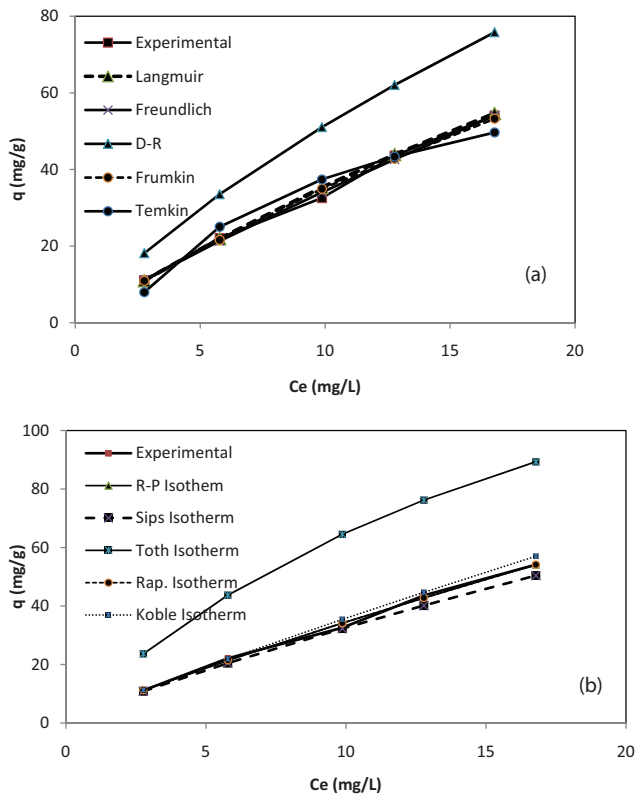

Fig. 8. Adsorption isotherm equations of CL. (a) Two parameters; (b) three parameters.

The Dubinin–Radushkevich isotherm for the adsorption of MB is presented in Figs. 7–10 at AC, CL, FA and PC, respectively. The values of E are 12.91, 9.11, 12.91 and 22.36 kJ/mol for MB at AC, CL, FA and PC, respectively. The typical range of bonding energy for ion-exchange mechanisms is 8–16 kJ/mol, indicating that chemical adsorption may play a significant role in the dye adsorption process [22]. Considering the error values of Dubinin–Radushkevich provided worse results than the results of other isotherms. D-R isotherm is considered as the best-fit isotherm equation for FA (Fig. 9).

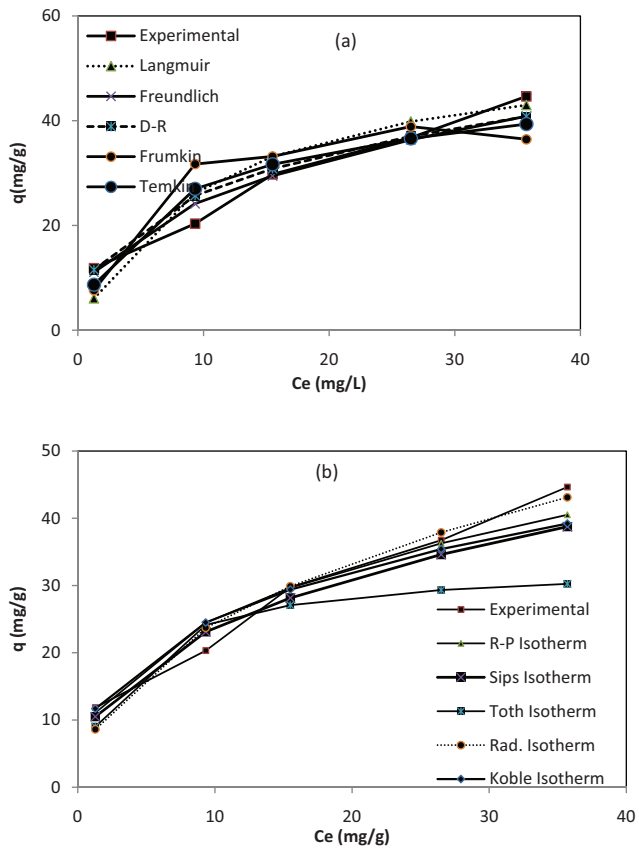

Fig. 9. Adsorption isotherm equations of FA. (a) Two parameters; (b) three parameters.

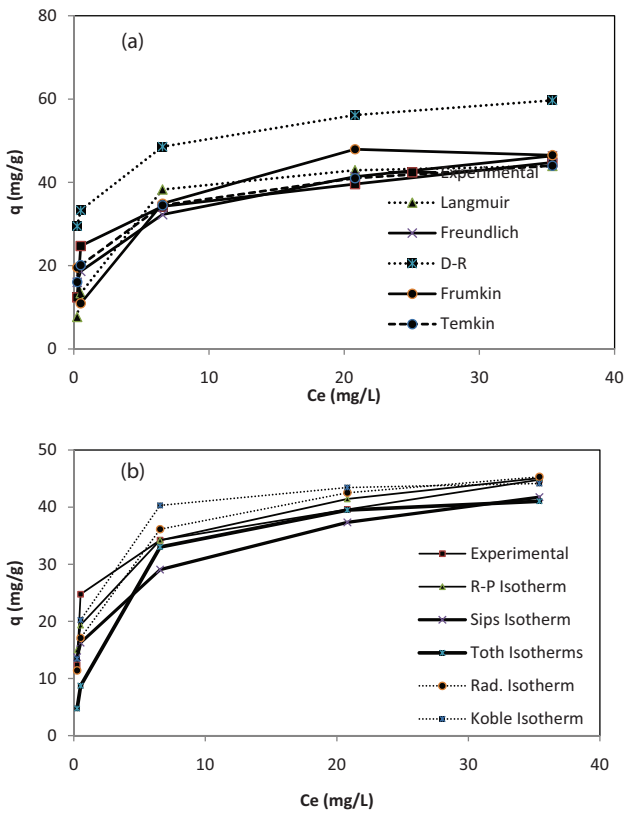

Fig. 10. Adsorption isotherm equations of PC. (a) Two parameters (b) three parameters.

The heat of adsorption and the adsorbate–adsorbate interaction on the adsorption isotherms were studied by Temkin. The adsorption data were analyzed according to the non-linear form of the Temkin isotherms are shown in Figs. 7–10 for MB at AC, CL, FA and PC, respectively. The equilibrium of the data indicates that the Temkin isotherm is close to dye adsorption data.

The Frumkin equation has been specially developed to add to the account the lateral interactions that occur on the surface. The Frumkin isotherm constants and value of error functions are summarized in Table 2. The constant k is related to the adsorption equilibrium.

$$\ln k = \frac{-\Delta G}{RT} \tag{4}$$

The negative values of free energy of ΔG indicate the feasibility of the adsorption process and its spontaneous nature. The values of ΔG are −22.77, −15.37, −24.55 and −34.84 kJ/mol for MB at AC, CL, FA and PC, respectively.

R-P isotherm is a hybrid isotherm featuring both Langmuir and Freundlich isotherms [23]. This equation is reduced to a Langmuir isotherm when $\beta = 1$ and a linear isotherm in the case of low surface coverage. Typically, a minimization procedure has been adopted to solve the equations by maximizing the correlation coefficient between the experimental data points and Microsoft Excel's solvent add-on function and the theoretical model estimates.

The Redlich–Peterson (R-P) isotherm plots for adsorption of MB are presented in Figs. 7–10 for AC, CL, FA and PC, respectively. Examination of the sources shows that the isotherm results of MB are close to the experimental results. The R-P isotherm constants K_R, a_R and β and values of error analysis for adsorbents presented in Table 2. As in the respective figures, the error analysis values are small for CL.

Sips isotherm is a combination of the Langmuir and Freundlich isotherms. At low dye concentrations, the Sips isotherm is reduced to the Freundlich isotherm. Isotherm at high concentrations provides Langmuir isotherm. Table 2 shows the values of the Sips isotherm constants and values of error analysis. With increasing K_s value, the error value (Δq) is reduced. The clay was also seen, as the least error (6.57%) is in the Redlich–Peterson isotherm.

Toth isotherm is useful in describing heterogeneous adsorption systems. Its correlation presupposes an asymmetrical quasi-Gaussian energy distribution with a widened left-hand, that is, most sites have adsorption energy less than the mean value [24]. The error values for the Toth isotherm are higher than for all isotherms. Suggesting that the Toth isotherm is homogeneous in adsorption with the dye if considered to be effective for heterogeneous structures.

The model exponent of Radke–Prausnitz is represented by p, where K_{Rp} and k_{Rp} are shown in Table 2. The maximum adsorption capacity (K_{Rp}) value found for the Radke–Prausnitz isotherm for MB is lower than that found by Redlich–Peterson, Toth and Sips isotherms.

Koble–Corrigan isotherm is another three-parameter empirical model for dyes adsorption. It is a combination of the Langmuir and Freundlich isotherm type models. The corresponding Koble–Corrigan constants and error analysis for MB are given in Table 2. The constants *n* are near to 1, and these indicate the isotherm for MB is approaching to Langmuir form for all adsorbents.

4. Conclusion

The results obtained from the present study can be summarized as follows:

- XRD peaks for PC are indicative of highly organized crystalline cellulose. Clay has got prominent peaks assigned to kaolinite, quartz in XRD diffractogram.
- According to initial concentration of MB that the highest adsorption capacity was seen in PC.
- The adsorption capacities decreases in the following order: clay > AC > FA > PC. This change is due to the difference in the surface properties of the adsorbents.
- Langmuir, Freundlich, Dubinin–Radushkevich, Temkin, and Frumkin equations were used to illustrate the adsorption of MB with different adsorbents. The Langmuir and Freundlich models denote a better value of correlation coefficient than the other models in the studied.
- The adsorption of MB with different adsorbents was found to be endothermic and spontaneous according to the results revealed by the Temkin and Frumkin isotherms.
- The three-parameter Redlich–Peterson isotherm equation was found to provide the closest fit to the equilibrium data and the optimum parameter values were produced by non-linear regression.

References

[1] Y. Zhou, L. Zhang, Z. Cheng, Removal of organic pollutants from aqueous solution using agricultural wastes: a review, J. Mol. Liq., 212 (2015) 739–762.

[2] H.A. Hegazi, Removal of heavy metals from wastewater using agricultural and industrial wastes as adsorbents, HBRC J., 9 (2013) 276–282.

[3] A. Mittal, R. Ahmad, I. Hasan, Biosorption of Pb^{2+}, Ni^{2+} and Cu^{2+} ions from aqueous solutions by L-cystein-modified montmorillonite-immobilized alginate nanocomposite, Desal. Wat. Treat., 57 (2016) 17790–17807.

[4] A. Mittal, R. Ahmad, I. Hasan, Poly(methyl methacrylate)-grafted alginate/Fe_3O_4 nanocomposite: synthesis and its application for the removal of heavy metal ions, Desal. Wat. Treat., 57 (2016) 19820–19833.

[5] H. Javadian, F. Ghorbani, H. Tayebi, S. Asl, Study of the adsorption of Cd (II) from aqueous solution using zeolite-based geopolymer, synthesized from coal fly ash; kinetic, isotherm and thermodynamic studies, Arabian J. Chem., 8 (2015) 837–849.

[6] S. Azarkan, A. Peña, K. Draoui, C.I. Sainz-Díaz, Adsorption of two fungicides on natural clays of Morocco, Appl. Clay Sci., 123 (2016) 37–46.

[7] M. Hadi, M.R. Samarghandi, G. McKay, Equilibrium two-parameter isotherms of acid dyes sorption by activated carbons: study of residual errors, Chem. Eng. J., 160 (2010) 408–416.

[8] C. Shangbin, H. Yusuf, F. Changqin, Z. Han, Z. Yanming, Z. Zhaoxi, Micro and nano-size pores of clay minerals in shale reservoirs: implication for the accumulation of shale gas, Sediment. Geol., 342 (2016) 180–190.

[9] J.E. Boulingui, C. Nkoumou D. Njoya, F. Thomas, J. Yvon, Characterization of clays from Me Safe and Ngono (Ne-Libreville, Gabon) for potential uses in fired products, Appl. Clay Sci., 115 (2015) 132–144.

[10] M. Chi, Synthesis and characterization of mortars with circulating fluidized bed combustion fly ash and ground granulated blast-furnace slag, Constr. Build. Mater., 123 (2016) 565–573.

[11] I. Langmuir, The adsorption of gases on plane surfaces of glass, mica and platinum, J. Am. Chem. Soc., 40 (1918) 1361–1368.

[12] H.M.F. Freundlich, Über die adsorption in iösungen, Phys. Chem., 57 (1906) 385–470.

[13] M.M. Dubinin, L.V. Radushkevich, The equation of the characteristic curve of the activated charcoal, Proc. Acad. Sci. USSR Phys. Chem. Sect. 55 (1947) 331–337.

[14] M.J. Temkin, V. Pyzhev, Recent modifications to Langmuir isotherms, Acta Physiochim. Chem. USSR, 12 (1940) 271–279.

[15] Ç. Sarıcı Özdemir, Removal of methylene blue by activated carbon prepared from waste in a fixed-bed column, Part. Sci. Technol., 32 (2014) 311–318.

[16] O. Redlich, D.I. Peterson, A useful adsorption isotherm, J. Phys. Chem., 63 (1959) 1024–1026.

[17] R. Sips, Combined form of Langmuir and Freundlich equations, J. Chem. Phys., 16 (1948) 490–495.

[18] J. Toth, State equations of the solid gas interface layer, Acta Chem. Acad. Hung., 69 (1971) 311–317.

[19] K.V. Kumar, K. Porkodi, Isotherms and thermodynamics by linear and non-linear regression analysis for the sorption of methylene blue onto activated carbon: comparison of various error functions, J. Hazard. Mater., 151 (2008) 794–804.

[20] R.A. Kobl, T.E. Corrigan, Adsorption isotherm for pure hydrocarbons, Ind. Eng. Chem., 44 (1952) 383–387.

[21] Ç. Sarıcı-Özdemir, Y. Önal, Equilibrium, kinetic and thermodynamic of adsorption of environmental pollutant tannic acid onto activated carbon, Desalination, 251 (2010) 146–152.

[22] F. Kılıç, Ç. Sarıcı Özdemir, Experimental and modeling studies of methylene blue adsorption onto particles of peanut shell, Part. Sci. Technol., 34 (2016) 658–664.

[23] M. Belhachemi, F. Addoun, Adsorption of Congo red onto activated carbons having different surface properties: studies of kinetics and adsorption equilibrium, Desal. Wat. Treat., 37 (2012) 122–129.

[24] T.S. Anirudhan, P.G. Radhakrishnan, Kinetic and equilibrium modelling of cadmium(II) ions sorption onto polymerized tamarind fruit shell, Desalination, 249 (2009) 1298–1307.